Nuclear dependence of the Drell-Yan process in relativistic heavy ion collisions

Athanasios N. Petridis
Department of Physics and Astronomy, Iowa State University, Ames, Iowa 50011
(Received 1 October 1993)

The EMC-type effects observed in lepton, hadron-nucleus collisions have revised the conventional high energy picture of the nucleus as a collection of semi-independent nucleons interacting via a meson field. For high momentum transfers deviations from this picture can be accounted for by a QCD treatment in which the nuclear dependence, attributed to overlapping of bound nucleons, is introduced through the nonperturbative parton momentum distributions. These phenomena must be more pronounced in nucleus-nucleus interactions to be studied at the Relativistic Heavy Ion Collider. We calculate the ratio of the Drell-Yan cross section for collisions of two large nuclei to that for interactions of two protons or deuterium nuclei to order α_s. We predict that in the invariant mass range between the heavy quarkonium peaks this ratio is less (greater) than one for small (large) values of the pair longitudinal and transverse momentum. For fixed nucleon energy the depletion at low lepton momenta decreases with increase of the invariant mass and disappears well beyond the meson resonances. We investigate the dependence of these effects on the choice of ocean and gluon momentum distributions.

PACS number(s): 25.75.+r, 13.85.Qk, 12.38.Bx

I. INTRODUCTION

The production of lepton-antilepton pairs in high energy hadron collisions has been successfully attributed to the annihilation of a quark and an antiquark originating in the interacting hadrons to a virtual photon which subsequently decays into the lepton pair [1]. Within the framework of the quark-parton model the calculation of the lepton pair production rate due to this generally called Drell-Yan process relies on the fact that at high energies the cross section can be factorized into a parton level part which can be calculated perturbatively and nonperturbative distribution functions that express the combined probability for the interacting partons to carry given fractions of the hadron momenta. Application of QCD leads to corrections to the lowest order Drell-Yan cross section [2] without invalidating its factorizability [3]. Because of the involvement of antiquarks this process has been used to supplement deeply inelastic scattering data with lepton probes in order to extract the ocean quark distributions in hadrons since these distributions are accepted to be process independent.

Another potentially important correction to the Drell-Yan cross section comes into play when at least one of the reacting hadrons is a nucleon bound in a nucleus. Deeply inelastic scattering data with charged lepton probes on nuclei have conclusively shown that nucleons bound in the nucleus cannot be treated as independent constituents [4]. At small values of the Bjorken x_{Bj} variable the deep inelastic scattering cross section on a large nucleus is depleted relative to that on deuterium, treated as a loosely bound system of a proton and a neutron (shadowing), and is enhanced for large x_{Bj} (antishadowing). This effect has also been verified to appear in experiments using neutrino and antineutrino probes demonstrating thus its presence with the weak current [5]. More recently it has been observed even in the case of light nuclei probed using weak interactions [6]. In general this phenomenon, known as the European Muon Collaboration (EMC) effect exhibits a slow dependence on the mass number and is almost insensitive to the value of the momentum transfer in the kinematic region covered by the data. Based on these observations we must conclude that the EMC effect is an intrinsic property of the nucleus independent of the probe used for its study.

The origins of this phenomenon have not been thoroughly understood and are subject to serious debate and investigation. Many contributions have been examined including nucleon Fermi motion [7], rescaling of x_{Bj}, identified as the *bound* nucleon momentum fraction carried by the quarks [8], rescaling of the momentum transfer due to size alteration of bound nucleons relative to free ones [9], pions in the nuclear matter [10], recombination of partons from adjacent nucleons [11], overlapping of nucleons to form multiquark clusters [12], and others. Combinations of such models have also been proposed and studied [13].

Most of these contributions are applicable only in a certain range of x_{Bj} with the exception of the formation of multiquark clusters, known as the quark cluster model (QCM), which gives good agreement with the data for all x_{Bj} and for both electromagnetic and weak interactions [14]. This model may overlap with Fermi motion at large x_{Bj}, rescaling at intermediate x_{Bj}, and parton recombination at small x_{Bj}. Caution is, therefore, required to avoid double counting of nuclear effects upon addition of more than one contribution in the same x_{Bj} range [15].

Based on the above mentioned merit of the quark cluster model we believe it can be successfully used to include the EMC-type nuclear effects discussed here into processes involving relativistic heavy ions as we expect such effects to carry over to collisions of two nuclei.

The fundamental principle of the QCM relies on the quantum mechanical result that wave functions of nucleons bound in a nucleus may overlap to the extent of forming multiquark color singlets larger than nucleons with nonzero probability. This probability is calculable in the case of light nuclei by making use of realistic nuclear wave functions. Scaling arguments can be applied to derive good estimates for heavy nuclei as well [12]. Therefore, the state vector of the nucleus can be expanded on a complete basis of color singlet states characterized by the number of valence quarks they contain. This model can also be considered as a phenomenological approach to nuclear effects whose parameters are determined by fitting EMC data. In essence, the $3q$ (nucleon) and $6q$ cluster terms of the color singlet expansion with a suitable, *effective*, value of the six-quark cluster formation probability and a reasonable choice of quark momentum distributions in the clusters suffice to give a good representation of the EMC data.

The QCM has been successfully applied to the Drell-Yan process in hadron-nucleus collisions with proton and pion projectiles [16,17]. In agreement with the fixed target experiment data of Ref. [18] it predicts that the ocean quark distribution in the nucleus is depleted (shadowed) relative to that in a free nucleon for small values of the longitudinal momentum of the Drell-Yan lepton pair and enhanced (antishadowed) for large values. These deviations from the free nucleon results are balanced in a way that the nuclear Drell-Yan cross section per unit mass number integrated over the lepton pair longitudinal momentum is very close to that of a nucleon. These studies have not, however, considered the lepton pair transverse momentum dependence of the cross section since they were restricted to the lowest order calculation.

The production of real photons in collisions of protons with heavy nuclei has also been studied within the QCM framework. It has been shown [17,19] that real photons with large transverse momenta should be produced more copiously in the case of heavy nuclear targets as a consequence of an EMC-type effect on the gluon distributions. Introduction of the model to the production of real photons in central heavy ion collisions has resulted in the prediction that the nuclear effects should be more dramatic in this case unveiling a very pronounced EMC-like behavior of the real photon rate [20]. This observation has led the author of this work to consider the implications of the QCM on the Drell-Yan process with relativistic heavy nuclei for all the variables determining the lepton pair phase space.

The calculation presented here refers to the initial hard scattering stage of the nucleus-nucleus collisions. It is believed that, at RHIC, the energy density in the interaction region will be high enough to allow for the formation of quark gluon plasma (QGP), a QCD phase in which quarks and gluons become unconfined. Upon the QGP phase transition the new state of matter is expected to radiate, among others, low transverse momentum real and virtual photons with thermal distributions superimposed on those originating in the initial (hard scattering) and final (π^0 decay, $\pi^{\pm}$ annihilation, and bremsstrahlung) stages of the heavy ion interaction [21]. If a state is at equilibrium its effective temperature can be characterized by the expectation value of the transverse momentum of the emitted radiation. In order to isolate the thermal (QGP) component of the radiation it is imperative to understand all other sources that may contribute to the real and virtual photon distributions, especially the initial hard scattering stage. In addition, the Drell-Yan process constitutes a background from which the quarkonium resonances must be extracted. In particular, the Υ particle which, due to its very small radius, is not seriously affected by final state interactions may carry important information from the state of matter in which it is produced [22]. Hence, its Drell-Yan background must be evaluated accurately, including nuclear effects, before possible modifications of its production rate due to the QGP transition can be inferred.

In Sec. II we give a brief description of our model, in Sec. III we present an outline of the calculations, in Sec. IV we show our results and discuss their physical meaning, and we conclude with some outlook in Sec. V.

II. ESSENTIALS OF THE QUARK CLUSTER MODEL

The quark cluster model (QCM) is based on the quantum mechanical expansion of the nuclear state of $3A$ valence quarks (A is the mass number of the nucleus) on a basis of color singlet states characterized by the number of valence quarks they contain (3 for a nucleon, 6 for a $6q$ cluster, and so on),

$$|A\rangle = \alpha|3q\rangle + \beta|6q\rangle + \gamma|9q\rangle + \cdots . \tag{1}$$

The squares of the magnitudes of the expansion coefficients express the probabilities for occurrence of the corresponding states in the nucleus in a dynamic equilibrium with one another. They have been calculated using nuclear wave functions and have been shown to decrease rapidly as the number of valence quarks in the singlet state increases [12]. In principle, the expansion (1) also contains pions as well as possible exotic pentaquark states but with much smaller probabilities. We will not discuss such contributions here. Therefore, we may truncate the right-hand side of Eq. (1) to the first two (or three) terms maintaining all its essential implications. If this approach is followed, the multiquark cluster probabilities are parameters to be determined by fitting the experimental data. In this work we use the first two terms and an *effective* six-quark cluster probability f. Then the nucleon probability is simply $1-f$. Because of the fact that the nuclear density is approximately constant for large nuclei we expect this probability to vary logarithmically with A,

$$f = k \ln A, \tag{2}$$

where the coefficient k ranges from 0.0575 to 0.0721 [17] as follows from EMC data. For deuterium this gives f_{D}

between 0.04 and 0.05 in agreement with data on backward hadron production in deeply inelastic scattering experiments [23]. The values obtained from Eq. (2) are consistent with those calculated using nuclear wave functions [24].

A $3q$ cluster is simply a proton (p) or a neutron (n). A $6q$ cluster may be formed by superposition of two protons (pp), two neutrons (nn), or a proton and a neutron (pn). Knowing f, the average number of each type of clusters, n_p, n_n, n_{pp}, n_{pn}, or n_{nn}, can be found employing simple conservation conditions for the baryon number, the electric charge, and the cluster formation probability and assuming that for large nuclei $n_p \propto Z$ (Z is the atomic number of the nucleus), $n_n \propto N \equiv (A-Z)$, $n_{pp} \propto Z^2$, $n_{pn} \propto 2ZN$, and $n_{nn} \propto N^2$ [20]. A solution that satisfies all these conditions is

$$n_p = \left(\frac{1-f}{1+f}\right) Z, \quad n_n = \left(\frac{1-f}{1+f}\right) N, \tag{3}$$

$$n_{pp} = \left(\frac{f}{1+f}\right) \frac{Z^2}{A}, \quad n_{pn} = \left(\frac{f}{1+f}\right) \frac{2ZN}{A}, \tag{4}$$

$$n_{nn} = \left(\frac{f}{1+f}\right) \frac{N^2}{A}.$$

Clearly, the total numbers of 3 and $6q$ clusters, n_3 and n_6, are proportional to $(1-f)$ and f, respectively. In the case of deuterium we take $n_6 = n_{pn}$.

The longitudinal parton momentum distributions in multiquark clusters parallel to a direction of a large momentum transfer are assumed to be simple functions of the fraction x of the cluster momentum carried by the parton in this direction (the parton intrinsic transverse momentum k_T is neglected in this discussion). In the Bjorken scaling limit they do not depend on the momentum transfer Q^2. The variable x is a relativistically invariant quantity identified as $x_{\rm Bj}$ in deeply inelastic scattering and ranges from 0 to 1 [25]. The general expressions for the parton distributions in nucleons are suggested by deeply inelastic scattering data and those in $6q$ clusters should have the same general properties. A protonlike cluster of N valence quarks contains $2N/3$ *up* (u) valence quarks whose momentum distribution is denoted by $U_N(x)$ and $N/3$ *down* (d) valence quarks quarks whose momentum distribution is $D_N(x)$. The *ocean* of the cluster consists of three species of *sea* quarks accompanied by an equal number of antiquarks to maintain electric charge neutrality. Here, we assume that u and d quarks and antiquarks in the ocean have identical distributions, $S_N(x)$, and that the *strange* sea distribution is $S_N(x)/2$. The total sea or *ocean* distribution is then $O_N(x) = 5S_N(x)$. The gluon distribution is denoted by $G_N(x)$. The assumed parametrizations of the momentum distributions in protonlike clusters are

$$U_N(x) = B_N^u \sqrt{x}(1-x)^{b_N^u}, \tag{5}$$

$$D_N(x) = B_N^d \sqrt{x}(1-x)^{b_N^d}, \tag{6}$$

$$S_N(x) = A_N(1-x)^{a_N}, \tag{7}$$

$$G_N(x) = C_N(1-x)^{c_N}. \tag{8}$$

The parton number densities, denoted by lowercase symbols, are obtained from the momentum distribution functions upon division by x. We also take $b_N^d = b_N^u + 1$ as a simple way to accommodate the drop of the neutron to proton deeply inelastic structure function ratio with $x_{\rm Bj}$. The parameters of these distributions can be determined by a number of reasonable assumptions listed here in order of decreasing confidence [14,20]: (1) normalization of the valence distributions, (2) momentum sum rule, (3) dimensional counting rules ($b_N^u = 2N-3$), (4) assumption that the ratio of the total momenta carried by gluons and ocean quarks is the same for all clusters and approximately equal to 1/5, and (5) assumption that the gluon $(1-x)$ exponent is smaller than or at most equal to that of the ocean. We will take $(b_3^u, a_3, c_3) = (3,9,6)$ (EMC data support the choice $a_3 = 9$) and $(b_6^u, a_6, c_6) = (9,11,10)$ as central values and will investigate the sensitivity of our results on the sea and gluon parameters. The poorly known gluon distributions play a dominant role in the production of real photons and charmonium resonances so that one would expect to develop a better understanding of their parameters by studying EMC-type effects in these processes [20].

We remark that the $6q$ distributions are softer (concentrated at lower values of x) than those of nucleons. The *total* momentum fraction of the cluster carried by a certain parton species can be found by integrating the corresponding momentum distribution over x. The total momentum fraction carried by the valence quarks, x^V, decreases with N. It is equal to 0.31 for $N = 3$ and 0.28 for $N = 6$. The ocean and gluon distributions are proportional to the total momentum fractions carried by those partons, i.e., $O_N(x) \propto x^O(1+a_N)$ and $G_N(x) \propto x^G(1+c_N)$. The total momentum fractions are not affected by the choice of a_N and c_N. Gluons carry 0.57 of the $3q$ and 0.60 of the $6q$ cluster momentum. It must be emphasized that in this model momentum is conserved within each cluster and within the nucleus as a whole.

The number of independent parameters needed to specify the parton distributions can be greatly reduced if relations among the distributions in clusters with the same isospin (I) are applied [17]. Such relations connect the neutron to the proton distributions ($I = 1/2$) in a straightforward way through the equations

$$U_p(x) = D_n(x) \equiv U_3(x), \tag{9}$$

$$D_p(x) = U_n(x) \equiv D_3(x).$$

The states pp and nn ($I = 1$) are related by the following formulas which are analogous to Eq. (9):

$$U_{pp}(x) = D_{nn}(x) \equiv U_6(x), \tag{10}$$

$$D_{pp}(x) = U_{nn}(x) \equiv D_6(x).$$

The $I = 1$ component of the pn state belonging to the same triplet with the pp state is also connected to it. We can assume that the $I = 0$ pn component has the same distributions as the isoprobable $I = 0$ one. These

remarks lead to the equations

$$U_{pn}(x) = D_{pn}(x) = [U_6(x) + D_6(x)]/2. \quad (11)$$

The sea and gluon distributions are taken to be independent of cluster isospin; therefore, they are the same for all clusters with N valence quarks.

III. CALCULATION OF THE CROSS SECTION

In this section we present a calculation of the lepton pair cross section in central heavy ion collisions to order α_s. At the level of interacting partons the processes that contribute to this cross section are represented by the Feynman diagrams shown in Fig. 1. The lowest order QED contribution (DY) is described by the well-known quark-antiquark annihilation diagram [Fig. 1(a)] in which a virtual photon is produced, subsequently decaying into a lepton pair. The quark-antiquark annihilation (A) diagrams involving an emitted gluon [Fig. 1(b)] and the quark-gluon Compton-type scattering (C) diagrams [Fig. 1(c)] are the order α_s corrections to it. We assume that the initial state partons move in the z direction defined by the colliding beams because their relatively small intrinsic transverse momentum can be neglected [25]. In this approximation the lowest order diagram cannot produce lepton pairs with nonzero transverse momentum. The pairs produced by the order α_s diagrams can have high transverse momentum balanced by that of a quark or gluon induced jet.

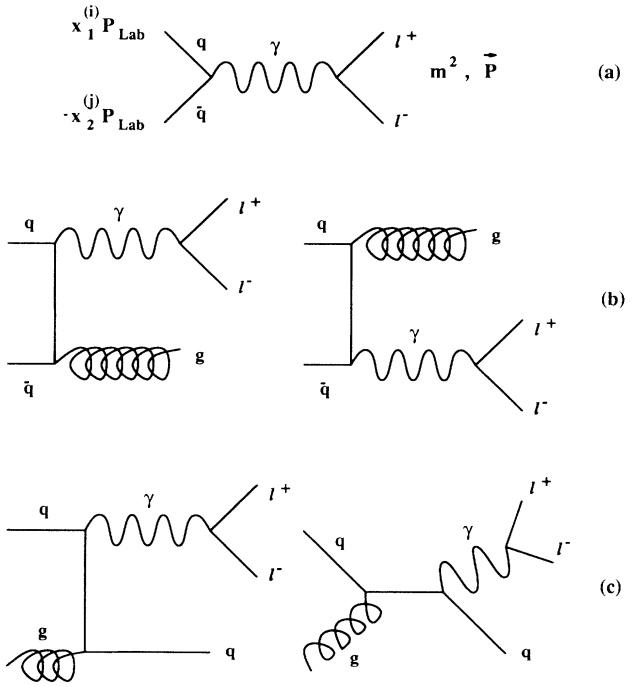

FIG. 1. Feynman diagrams contributing to the Drell-Yan lepton pair production. (a) Lowest order QED process. (b) Quark-antiquark annihilation to order α_s. (c) Quark-gluon Compton scattering to order α_s. The kinematics is defined in (a). One parton carries momentum fraction $x_1^{(i)}$ of the positively moving hadron momentum, and the other one carries $x_2^{(j)}$ of the negatively moving hadron momentum. Nucleons have momentum $\pm P_{\rm lab}$ and $6q$ clusters have momentum $\pm 2P_{\rm lab}$.

We denote the parton level variables using a symbol with a caret and the hadron level ones using the same symbol but without a caret. The quark clusters moving in the positive z direction carry momentum $P_1^{(i)} = (i/3)P_{\rm lab}$ and those moving in the opposite direction carry $P_2^{(j)} = -(j/3)P_{\rm lab}$, where i, j are equal to 3 for nucleons and 6 for $6q$ clusters and $P_{\rm lab}$ is the nuclear momentum per unit mass number. The cluster longitudinal momentum due to the Fermi motion is assumed to be an element of the quark cluster model [15] and is not included explicitly. The cluster transverse momentum will be neglected. We define the variables $n_1^{(i)} = i/3$ and $n_2^{(j)} = j/3$ which give the mass of the clusters in units of the nucleon mass and take on the values 1 and 2. The hadron level kinematic invariants expressed in laboratory (nucleon center of momentum) frame quantities are

$$s^{(i,j)} = 4n_1^{(i)} n_2^{(j)} P_{\rm lab}^2, \quad (12)$$

$$t^{(i)} = -2n_1^{(i)} P_{\rm lab}(E - p_z) + m^2, \quad (13)$$

and

$$u^{(j)} = -2n_2^{(j)} P_{\rm lab}(E + p_z) + m^2, \quad (14)$$

where p_z, E, and m are the longitudinal momentum, energy, and invariant mass of the lepton pair (virtual photon), respectively. The lepton pair momentum in the transverse direction is p_T. It must be pointed out that the values of the kinematic invariants *assumed* by the experimenters are those involving two colliding nucleons, i.e., $s \equiv s^{(3,3)}, t \equiv t^{(3)}$, and $u \equiv u^{(3)}$. Then

$$s^{(i,j)} = n_1^{(i)} n_2^{(j)} s, \quad (15)$$

$$t^{(i)} = n_1^{(i)} t + (1 - n_1^{(i)})\, m^2, \quad (16)$$

and

$$u^{(j)} = n_2^{(j)} u + (1 - n_2^{(j)})\, m^2. \quad (17)$$

Using the experimentally measured variables p_T, p_z, and E, the longitudinal (x_F) and the transverse (x_T) momentum fractions as well as the energy fraction (x_E) of the lepton pair are defined as

$$x_F \equiv \frac{2p_z}{\sqrt{s}} = \frac{p_z}{P_{\rm lab}}, \quad x_T \equiv \frac{2p_T}{\sqrt{s}} = \frac{p_T}{P_{\rm lab}}, \quad (18)$$

$$\text{and } x_E \equiv \frac{2E}{\sqrt{s}} = \frac{E}{P_{\rm lab}}.$$

The interacting parton that originates in the positively moving cluster carries a fraction $x_1^{(i)}$ of its parent hadron momentum and that coming from the negatively moving one carries a fraction $x_2^{(j)}$ [Fig. 1(a)]. Using this momentum fraction definition we can write the kinematic

invariants pertaining to the parton level interaction as

$$\hat{s}^{(i,j)} = x_1^{(i)} x_2^{(j)} s^{(i,j)}, \tag{19}$$

$$\hat{t}^{(i)} = x_1^{(i)} t + (1 - x_1^{(i)})\, m^2, \tag{20}$$

and

$$\hat{u}^{(j)} = x_2^{(j)} t + (1 - x_2^{(j)})\, m^2. \tag{21}$$

The parton level cross sections, including color factors, that correspond to the three contributing processes are [26]

$$\frac{d\hat{\sigma}_{\rm DY}^{(i,j)}}{dm^2 d\hat{t}^{(i)}} = \frac{4\pi\alpha^2}{9\hat{s}^{(i,j)}} \delta\left(\hat{s}^{(i,j)} - m^2\right) \delta\left(\hat{t}^{(i)}\right), \tag{22}$$

$$\frac{d\hat{\sigma}_{A}^{(i,j)}}{dm^2 d\hat{t}^{(i)}} = \frac{8\alpha^2\alpha_s(Q^2)}{27m^2(\hat{s}^{(i,j)})^2} \left[\frac{\hat{t}^{(i)}}{\hat{u}^{(j)}} + \frac{\hat{u}^{(j)}}{\hat{t}^{(i)}} - 2m^2 \times \left(\frac{1}{\hat{u}^{(j)}} + \frac{1}{\hat{t}^{(i)}} \right) + \frac{2m^4}{\hat{t}^{(i)}\hat{u}^{(j)}} \right], \tag{23}$$

and

$$\frac{d\hat{\sigma}_{C}^{(i,j)}}{dm^2 d\hat{t}^{(i)}} = -\frac{\alpha^2\alpha_s(Q^2)}{9m^2(\hat{s}^{(i,j)})^2} \left[\frac{\hat{s}^{(i,j)}}{\hat{u}^{(j)}} + \frac{\hat{u}^{(j)}}{\hat{s}^{(i,j)}} + \frac{2m^2\hat{t}^{(i)}}{\hat{s}^{(i,j)}\hat{u}^{(j)}} \right]. \tag{24}$$

These cross sections must be weighted with the square of the electric charge of the involved quarks. When $m^2 = 0$ the A and C cross sections reduce to those for real photon production after removal of the lepton multiplicative factor $[\alpha/(3\pi m^2)]$ [20]. For three active quark flavors the strong coupling constant is $\alpha_s(Q^2) = (12\pi/27)/\ln\left(\frac{Q^2}{\Lambda^2}\right)$. The variable Q^2 must be related to p_T^2 since, to this order, this is the only scale in the problem. The A and C diagrams are partially responsible for the Altarelli-Parisi type evolution of the parton distribution functions since one of the partons that produce the virtual photon can be thought of as the product of splitting of the parton that originates in the interacting hadron. Therefore, we can use x-scaling parton distributions and include the A and C terms to partially account for their evolution [2]. Because the A and C diagrams give both a part of the parton distribution evolution and the virtual photon transverse momentum to the same order we shall make the identification $Q^2 = p_T^2$. The exact value of the QCD renormalization constant Λ plays only a minor role when ratios of cross sections are considered. However, $\ln(\Lambda^2)$ does not completely cancel to this order, contrary to the case of real photon production, because of the presence of the lowest order QED term. We shall take $\Lambda = \Lambda_{\overline{\rm MS}} = 100$ MeV. It may be interesting to note that the numerical values of the parton level kinematic variables and cross sections do not depend on the type of colliding clusters for given x_F, x_T, and m^2.

In order to obtain the hadron level cross sections we first use the convenient transformation

$$\frac{E\, d\hat{\sigma}_{{\rm DY},A,C}^{(i,j)}}{dm^2 d^3p} = \frac{\hat{s}^{(i,j)}}{\pi} \frac{d\hat{\sigma}_{{\rm DY},A,C}^{(i,j)}}{dm^2 d\hat{t}^{(i)}} \delta\left(\hat{s}^{(i,j)} + \hat{t}^{(i)} + \hat{u}^{(j)} - m^2\right), \tag{25}$$

where p is the virtual photon three-momentum. Then, assuming factorization, we convolute the parton level cross sections with appropriate distribution functions expressing the combined probabilities for the parton from one cluster to carry momentum fraction $x_1^{(i)}$ and the parton from the second cluster to carry momentum fraction $x_2^{(j)}$. These functions are sums of products of parton *density* distributions weighted by the squares of the quark charges. We denote the four functions pertaining to the quark-antiquark annihilation, used in the calculation of both the DY and the A terms, by $H_{q\bar{q}}^{(i,j)}(x_1^{(i)}, x_2^{(j)})$ and the other four needed for the C term by $H_{qg}^{(i,j)}(x_1^{(i)}, x_2^{(j)})$. As an example, the quark-antiquark annihilation function in the case of a collision of 3 with $6q$ clusters contains a term

$$n_6 \left[\left\{ \tfrac{4}{9} n_p + \tfrac{1}{9} n_n \right\} u_3(x_1^{(3)}) + \left\{ \tfrac{1}{9} n_p + \tfrac{4}{9} n_n \right\} d_3(x_1^{(3)}) + \tfrac{7}{6} n_3 s_3(x_1^{(3)}) \right] s_6(x_2^{(6)})$$

in which valence and sea quarks from the positively moving nucleons annihilate sea quarks from negatively moving $6q$ clusters. The isospin relations of Eqs. (9), (10) and (11) have been used to simplify this expression and the cluster numbers have been calculated using Eqs. (3) and (4). Complete expressions for the distributions $H_{q\bar{q}}^{(i,j)}(x_1^{(i)}, x_2^{(j)})$ and $H_{qg}^{(i,j)}(x_1^{(i)}, x_2^{(j)})$ are given in Ref. [20]. The convolution of these functions with the parton level cross sections involves a double integration over the momentum fractions of the interacting partons. Because of the presense of the δ function in Eq. (25) one set of these integrations can be trivially done. We choose to perform the $x_2^{(j)}$ integrations in this way. This yields the following relation between $x_1^{(i)}$ and $x_2^{(j)}$:

$$x_2^{(j)} = -\frac{x_1^{(i)}(t^{(i)} - m^2) + m^2}{x_1^{(i)} s^{(i,j)} + u^{(j)} - m^2}. \tag{26}$$

It also moves the lower limits of the $x_1^{(i)}$ integrations from 0 to

$$x_{1(\rm min)}^{(i)} = \frac{-u^{(j)}}{s^{(i,j)} + t^{(i)} - m^2}. \tag{27}$$

After performing the convolution the hadron level cross sections for the four types of collisions involving 3 and $6q$ clusters (characterized by the four combinations of i and

j) can be written as

$$\frac{E\,d\sigma^{(i,j)}_{\mathrm{DY},A,C}}{dm^2d^3p} = \int_{x^{(i)}_{1(\min)}}^{1} dx_1^{(i)}\, H^{(i,j)}_{q\bar{q},qg}(x_1^{(i)}, x_2^{(j)}) \times F^{(i,j)}\, \frac{\hat{s}^{(i,j)}}{\pi}\, \frac{d\hat{\sigma}^{(i,j)}_{\mathrm{DY},A,C}}{dm^2d\hat{t}^{(i)}}, \tag{28}$$

where

$$F^{(i,j)} = \frac{1}{x_1^{(i)}s^{(i,j)} + u^{(j)} - m^2} \tag{29}$$

is a remainder of the δ function.

We note that in the case of the DY term the presense of the δ function over m^2 trivializes the $x_1^{(i)}$ integrations as well and fixes the relation of the quark momentum fractions with the measured quantities by the equations

$$x_1^{(i)} = \frac{1}{2n_1^{(i)}}\left[\pm\sqrt{x_F^2+4\tau}+x_F\right] \quad \text{(only in DY)}, \tag{30}$$

$$x_2^{(j)} = \frac{1}{2n_2^{(j)}}\left[\pm\sqrt{x_F^2+4\tau}-x_F\right] \quad \text{(only in DY)}, \tag{31}$$

where $\tau = m^2/s$ and $x_F = n_1^{(i)}x_1^{(i)} - n_2^{(j)}x_2^{(j)}$ in this case.

Next we perform successive variable transformations resulting in

$$\frac{d\sigma^{(i,j)}_{\mathrm{DY},A,C}}{dm^2dx_Fdp_T^2} = \frac{\pi}{x_E}\,\frac{E\,d\sigma^{(i,j)}_{\mathrm{DY},A,C}}{dm^2d^3p}. \tag{32}$$

In order to obtain p_T-independent results we integrate over p_T^2. Because the A and C terms are infrared divergent we regularize the integrals with a cutoff $p^2_{T(\min)}$, which we take in the vicinity of 0.1 GeV^2. The strong coupling constant evaluated at this cutoff is 0.61, a rather large value. However, we will still apply perturbation theory in this limit keeping in mind that higher order corrections may become important as p_T approaches its imposed lower bound. On the other hand, if these corrections result in a multiplicative factor (K factor) [27] that is approximately independent of the lepton pair kinematic variables, they will mostly cancel when cross section *ratios* are computed. After performing the p_T^2 integration we sum over all the combinations of colliding clusters and obtain

$$\frac{d\sigma_{\mathrm{DY},A,C}}{dm^2dx_F} = \sum_{i,j=3,6}\int_{p^2_{T(\min)}}^{[p_T^{(i,j)}]^2_{(\max)}} dp_T^2\,\frac{d\sigma^{(i,j)}_{\mathrm{DY},A,C}}{dm^2dx_Fdp_T^2}. \tag{33}$$

In the case of the DY term this last integration eliminates the δ function over $\hat{t}^{(i)}$. The upper integration limit is determined by the kinematics, depending on the types of colliding clusters, and is equal to

$$[p_T^{(i,j)}]^2_{(\max)} = (4n_1^{(i)}n_2^{(j)} - x_F^2)\,P^2_{\mathrm{lab}} - m^2. \tag{34}$$

Finally we sum the DY, A, and C terms to obtain the lepton pair production cross section

$$\frac{d\sigma}{dm^2dx_F} = \frac{d\sigma_{\mathrm{DY}}}{dm^2dx_F} + \frac{d\sigma_A}{dm^2dx_F} + \frac{d\sigma_C}{dm^2dx_F}. \tag{35}$$

Our main interest is to study the EMC-type nuclear effects in the Drell-Yan lepton pair production. In order to isolate the nuclear dependence we can calculate the ratio of the cross section per unit mass number for two heavy nuclei to that for two light ones. Since we expect the nuclear effects to be more pronounced in the case of heavy nuclei, such ratios may exhibit interesting behavior. We, thus, define

$$R^{[A_1/A_2]} = \frac{1}{A^2}\,\frac{d\sigma^{(A_1)}}{dm^2dx_F}\left[\frac{d\sigma^{(A_2)}}{dm^2dx_F}\right]^{-1} \tag{36}$$

IV. RESULTS AND DISCUSSION

Following the steps outlined in the previous section we can numerically evaluate the cross section ratio defined by Eq. (36) and investigate its sensitivity to the various parameters of the model. The results we present here are calculated for $P_{\mathrm{lab}} = 100$ GeV per unit mass number which corresponds to the expected energy at the Relativistic Heavy Ion Collider (RHIC).

In order to develop some quantitative understanding of the influence of the A and C corrections to the lowest order Drell-Yan cross section ratio we first calculate this ratio using only the DY term (R_{DY}). In Fig. 2 we show the gold to proton cross section ratio for $m = 1$ GeV plotted versus positive x_F. In this case $n_1^{(i)}x_1^{(i)} > n_2^{(j)}x_2^{(j)}$ and the contribution of the negatively moving clusters dominates. It can be immediately observed that the shape of R_{DY} is remarkably similar to that of the EMC ratio, i.e., staring from a value below 1, it increases reaching a local maximum, then it decreases for intermediate momentum fractions, and, finally, increases again steeply reaching values well above 1. However, its depletion from unity at low x_F is much more pronounced than that of the EMC ratio. For comparison we show the results for $f_{\mathrm{Au}} = 0$ and for the two limiting values of $f_{\mathrm{Au}} = 0.30$ and 0.38 predicted by our model. It can be noted that in the absence of multiquark cluster contributions the ratio is lower than unity. This is a consequence of the nonisoscalarity of the heavy nucleus. A nucleus with more neutrons than protons contains more d than u valence quarks. Since the d quark distribution decreases with x more rapidly than that of the u quarks, the valence contribution to the cross section per unit A for nonisoscalar nuclei is reduced compared to that of protons. For $f = 0$ the ratio $R_{\mathrm{DY}}^{[A/p]}$ is a linear function of the nonisoscalarity $\epsilon = (N-Z)/(N+Z)$ of the nucleus. We can also observe that the effect of the mere presence of $6q$ clusters is more important than the exact value of f_{Au}.

The depletion of R_{DY} below unity for $x_F < 0.6$ is a result of the softer parton distributions in the $6q$ clusters. In the limit $m^2/s \to 0$ we can easily derive a simple

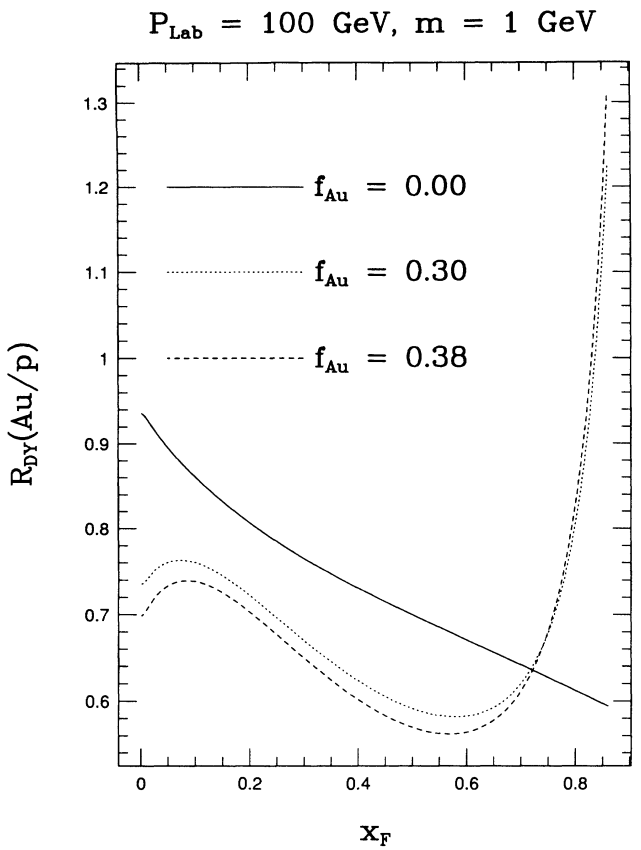

FIG. 2. The ratio of the Au to p cross sections per unit mass number versus the lepton pair longitudinal momentum fraction (x_F) for three values of the $6q$ cluster probability ($f_{\rm Au}$). The EMC-like behavior is more pronounced than in the case of hadron-nucleus collisions [17].

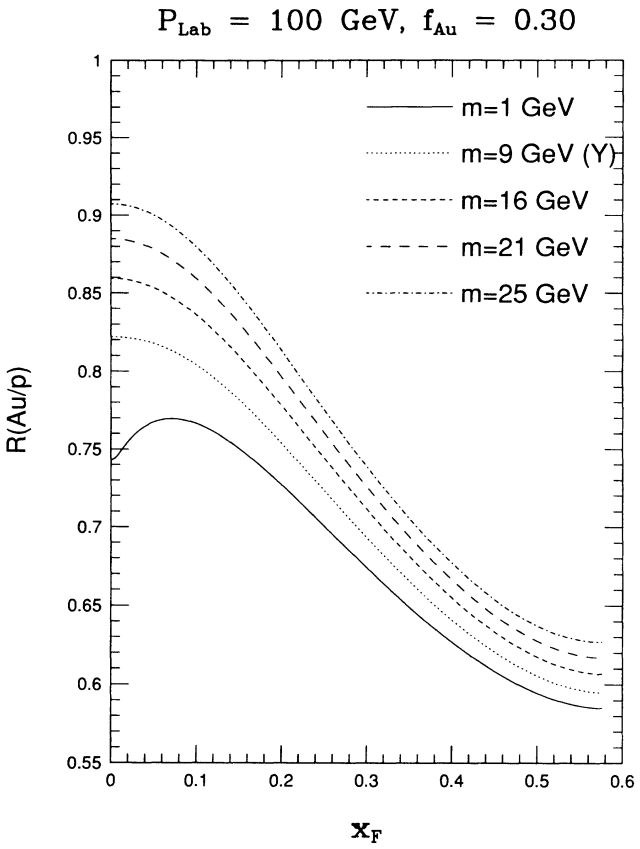

FIG. 3. Ratio of Au to proton lepton pair production cross sections for various fixed values of the lepton pair invariant mass (m) versus the lepton pair longitudinal momentum fraction (x_F). The curve corresponding to the Drell-Yan background of Υ is included. The $6q$ cluster probability ($f_{\rm Au}$) is 0.30.

expression for $R_{\rm DY}^{[A/p]}$ at $x_F = 0$,

$$R_{\rm DY}^{[A/p]}(0) \approx \left[\left(\frac{1-f}{1+f}\right) + \left(\frac{f}{1+f}\right)\left(\frac{A_6}{A_3}\right)\right]^2, \quad (37)$$

where $A_{3,6} = x_{3,6}^S(a_{3,6}+1)$ are the sea quark normalization factors for 3 and $6q$ clusters, respectively. In this limit the valence quark contribution is negligible and the ratio is essentially determined only by the shape of the sea distributions and the total fraction of the cluster momentum carried by them. The large increase above 1 in the limit $x_F \to 1$ can also be easily understood when $m^2/s \to 0$. In this case we can see that $x_2^{(j)} = 0$ while $x_1^{(i)} = 3/i$. The $3q$ cluster momentum distributions from the positively moving nucleus are, then, zero and the $6q$ cluster ones are finite. Consequently the cross-section ratio in which the numerator (denominator) is proportional to the $6q$ ($3q$) cluster *momentum* distributions diverges in this limit. We can, thus, state that this divergence is a phase space effect due to the fact that the $6q$ clusters are twice as massive as nucleons and, as a result, allow for more copious production of virtual photons.

Next we turn on the A and C terms and repeat the calculation. In Figs. 3 and 4 we plot $R^{[\rm Au/p]}$ versus x_F in the range (0, 0.6) for various values of m and for $f_{\rm Au} = 0.30$ and 0.38, respectively. We first observe that the cross section ratio including A and C corrections remains very close to that calculated using only the DY term. This suggests that QCD corrections cancel in cross section ratios so that even the lowest order calculation of R is reliable. Since we have introduced an infrared cutoff to regularize the integral over the transverse momentum, we must investigate the stability of the results to the choice of $p_{T(\rm min)}^2$. Our calculations have shown that R is indeed very stable even for values of $p_{T(\rm min)}^2$ approaching Λ^2. We observe that increasing m increases $R^{[\rm Au/p]}$. The reason for this is that as m becomes larger the momentum fraction $x_2^{(j)}$ increases and the $6q$ cluster distributions being softer than those of nucleons contribute less to the cross section. This leads to another interesting result. A comparison of Fig. 3 with Fig. 4 shows that further increase in $f_{\rm Au}$ slightly enhances $R^{[\rm Au/p]}(0)$ when m exceeds 16 GeV, contrary to what happens for $m < 16$ GeV, because the importance of the $6q$ cluster contribution increases with f but its actual numerical value decreases with m. A curve approximately indicating the Drell-Yan background to the Υ cross section is included in Figs. 3 and 4 to underline the necessity for a good estimation of

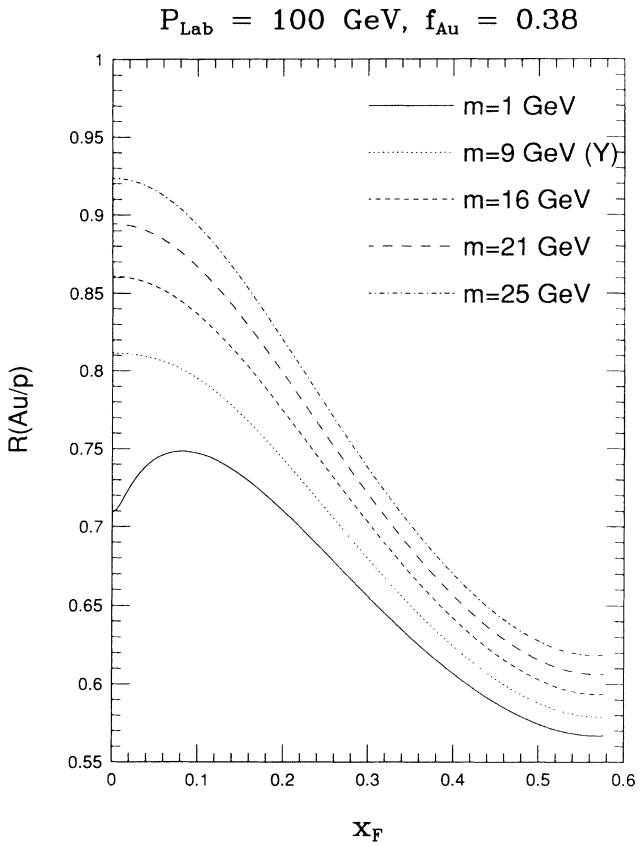

FIG. 4. Ratio of Au to proton lepton pair production cross sections for various fixed values of the lepton pair invariant mass (m) versus the lepton pair longitudinal momentum fraction (x_F). The curve corresponding to the Drell-Yan background of Υ is included. The $6q$ cluster probability ($f_{\rm Au}$) is 0.38.

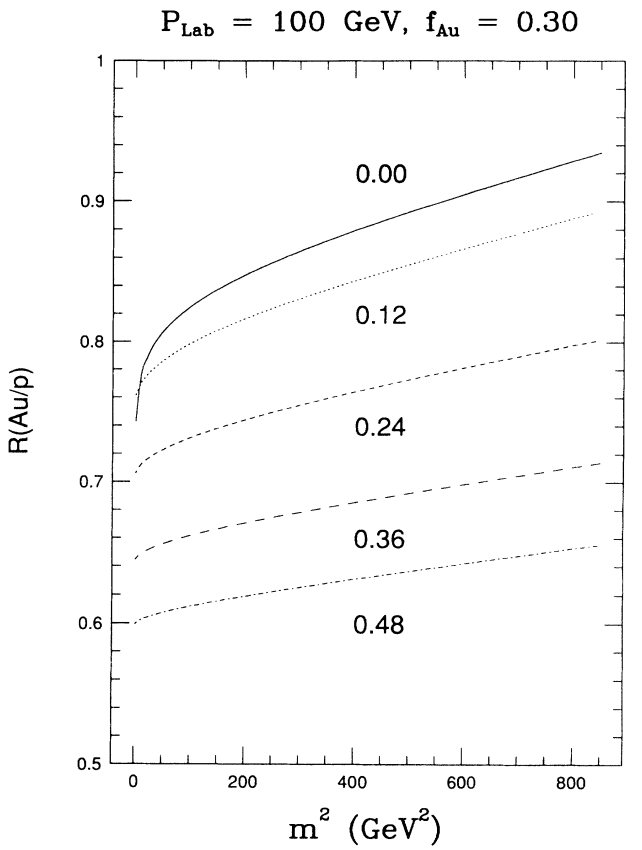

FIG. 5. Ratio of the Au to proton lepton pair production cross sections for various values of the lepton pair longitudinal momentum fraction (x_F, shown near the curves) versus the square of the lepton pair invariant mass (m^2). The $6q$ cluster probability ($f_{\rm Au}$) is 0.30.

the lepton pair production rate in order to extract the correct value of the bottomonium peak.

The dependence of $R^{[\rm Au/p]}$ on the invariant mass squared for various values of the longitudinal momentum fraction and the two limiting values of $f_{\rm Au}$ is shown in Figs. 5 and 6 in which the slow rise as m^2 increases becomes clear.

The influence of the nonisoscalarity of the heavy nucleus can be further elucidated by calculating the ratio $R^{[\rm Au,Ca/d]}$ in which the deuterium cross section in the denominator contains both neutron and $6q$ cluster contributions while the cross section in the numerator refers to either a nonisoscalar (Au) or an isoscalar (Ca) nucleus. In Fig. 7 we plot this ratio versus x_F for the two limiting combinations of the $6q$ cluster probabilities for deuterium and the heavy nucleus. We can observe that the depletion of the ratio below unity becomes more pronounced as the mass number increases. This is a direct result of the A dependence of the $6q$ cluster probability. The presence of the neutron in deuterium removes part of the effect initially shown in Fig. 2. The curves start increasing for lower x_F values than in the case of protons in the denominator. In Fig. 8 we show that, as a function of m^2, $R^{[A/d]}$ increases more steeply than $R^{[A/p]}$.

The poorly known sea and gluon distributions introduce an additional uncertainty in the model especially because in their experimental derivation from data using nuclei, EMC-type effects are not always accounted for. We must, therefore, examine the theoretical uncertainty in these distributions and compare it to that due to f. In our model sea quarks and gluons in nuclei behave in essentially the same manner, i.e., when the nuclear gluons are depleted relative to those of the proton the nuclear sea quarks follow their example. As indicated by Eq. (37) we can expect that a less depleted ratio should correspond to harder $3q$ cluster distributions (smaller a_3, c_3) accompanied by softer $6q$ cluster ones (larger a_6, c_6). This is shown in Fig. 9 in which the sea and gluon exponents are varied by one unit in either direction. It is clear that the uncertainty due to the choice of distributions is larger than that introduced by f. This conclusion holds for all values of the lepton pair invariant mass.

The transverse momentum behavior of the cross section ratio is another interesting phenomenon to discuss. To obtain this result we calculate the cross sections and from them R without integrating over p_T^2. The ratios $R^{[A/p]}$ and $R^{[A/d]}$ are plotted in Fig. 10 for $m = 1$ GeV and $x_F = 0$ as functions of x_T. It can be observed that

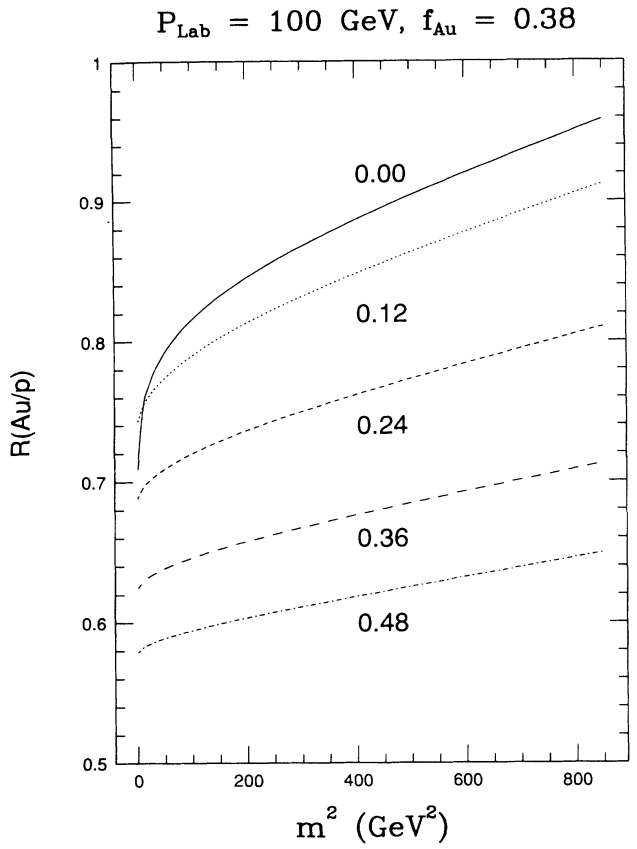

FIG. 6. Ratio of the Au to proton lepton pair production cross sections for various values of the lepton pair longitudinal momentum fraction (x_F, shown near the curves) versus the square of the lepton pair invariant mass (m^2). The $6q$ cluster probability (f_{Au}) is 0.38.

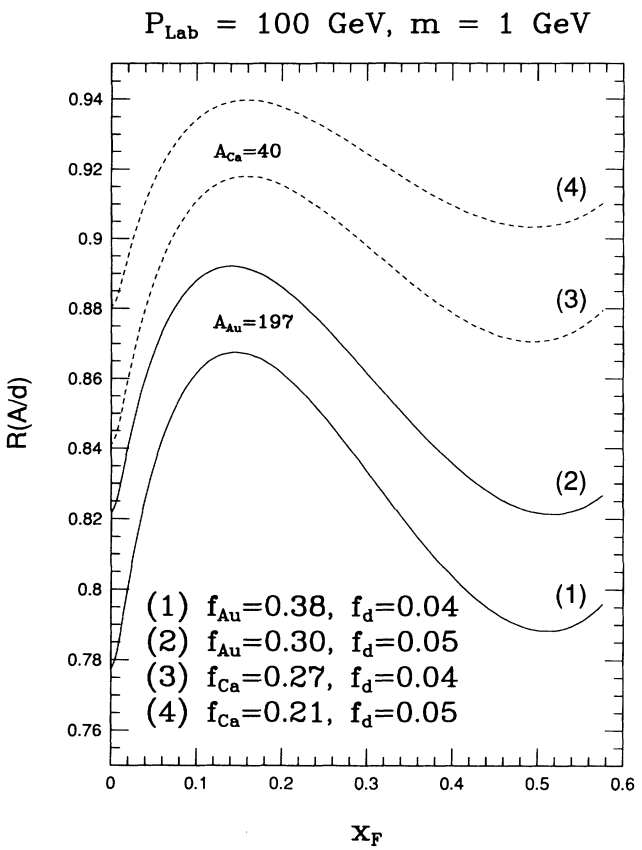

FIG. 7. The lepton pair production ratio $R^{[A/d]}$ for ^{197}Au and ^{40}Ca to deuterium. Increase in the mass number (A) produces more pronounced nuclear effects due to the increase in the $6q$ cluster probability f. R is plotted versus the longitudinal momentum fraction (x_F) of the lepton pair for fixed invariant mass (m).

for $x_T < 0.6, 0.5$, respectively, the ratios are lower than unity and they greatly exceed 1 for high transverse momenta. Another feature becomes apparent in Fig. 10. The ratio $R^{[A/p]}$ tends to infinity as $x_T \to 1$ but $R^{[A/d]}$ flattens out and tends to a constant value (approximately 30). This interesting behavior is easily understood upon considering that the major contribution from the $3q$ cluster momentum distributions comes for $x_{1,2}^{(3)} = x_T$ while that from $6q$ clusters comes for $x_{1,2}^{(6)} = x_T/2$. As a result the denominator of $R^{[A/p]}$ vanishes in the $x_T \to 1$ limit while that of $R^{[A/d]}$ remains finite beyond this value. Numerical calculations show that $R^{[A/p,d]}$ scales in x_T for different values of m^2, if x_F is fixed.

Finally we compute the exponent α (not to be confused with the fine structure constant) defined by the equation

$$\frac{d\sigma^{(A)}}{dm^2} = [A^2]^{\alpha} \frac{d\sigma^{(p)}}{dm^2}. \tag{38}$$

Based on the earlier observation that the A and C terms do not drastically affect the longitudinal dependence of the cross section ratio we use only the DY term to compute α. This requires integrations over x_F whose limits depend on the type of clusters involved in the interaction. For example, if $i = 3$ and $j = 6$, x_F varies in the range $(-2, 1)$. It is, thus, necessary to perform these integrations before the cluster summation prescribed by Eq. (35). Including the uncertainties in f and in the distribution exponents described earlier we present our results for α in Table I. It is interesting to note that α increases with A. The reason for this is the fact that when f increases R decreases for low x_F but increases sharply for high x_F and the area below the R curve in the high x_F region is larger. Therefore the x_F-integrated nuclear effect is more pronounced for lighter nuclei. However, the dependence of α on the nucleus is not very strong and consequently not easily observable even though Table I shows that an overall depletion of the nuclear cross section should be expected. Our calculations have shown that the exponent α almost does not depend on the value of m^2.

The correction introduced by the A and C terms is only a few percent of the total cross section and does not account for the experimental value of the Drell-Yan K factor [27,28] defined as the ratio of the cross section including higher order corrections (HOC's) to the leading

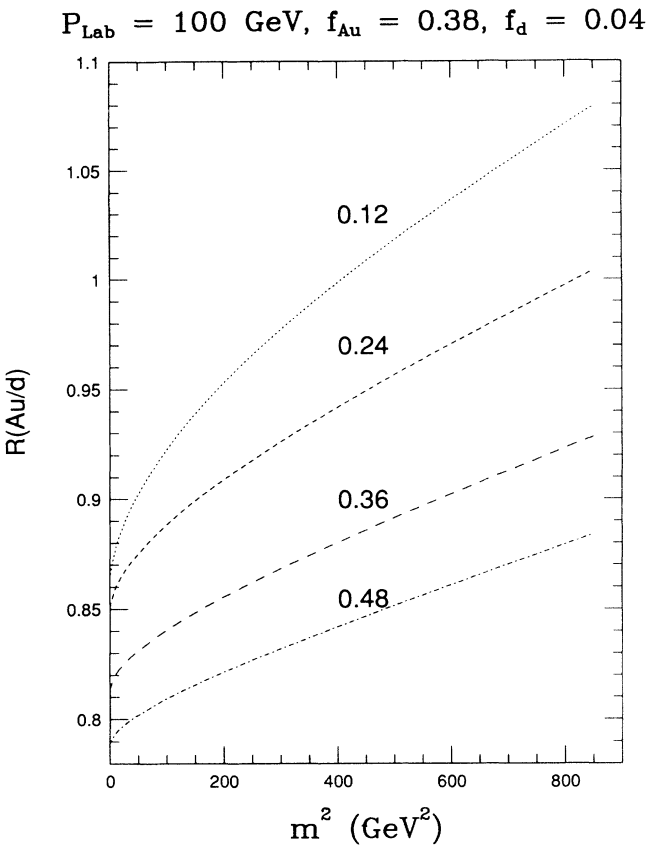

FIG. 8. Ratio of the Au to deuterium lepton pair production cross sections for various values of the lepton pair longitudinal momentum fraction (x_F, shown near the curves) versus the square of the lepton pair invariant mass (m^2). The $6q$ cluster probabilities are $f_{\rm Au} = 0.38$ and $f_d = 0.04$.

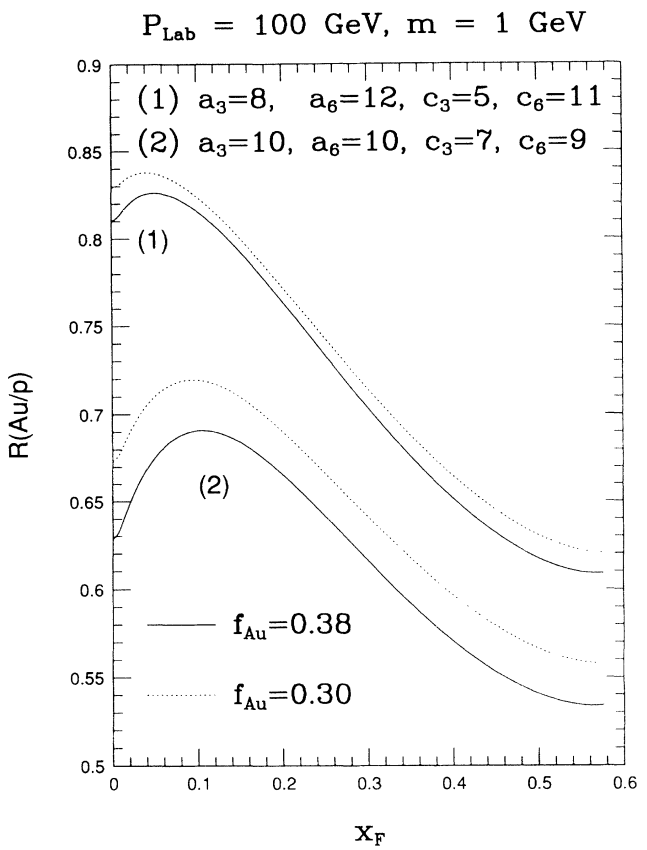

FIG. 9. Dependence of ratio of the Au to proton lepton pair production rate on the choice of exponents in the ocean ($a_{3,6}$) and gluon ($c_{3,6}$) distributions in 3 and $6q$ clusters for the two limiting values of the $6q$ cluster probability ($f_{\rm Au}$).

logarithm cross section calculated here. A more complete analysis is needed in order to determine possible nuclear effects on K. We can say, however, that even if the K factor in nucleus-nucleus collisions, $K^{(A)}$, is constant, its value might be different from that measured in proton-proton collisions, $K^{(p)}$. This can be seen upon relating the two factors through the formula

$$K^{(A)} = \frac{R_{\rm HOC}^{[A/p]}}{R^{[A/p]}} K^{(p)}, \tag{39}$$

where $R_{\rm HOC}^{[A/p]}$ is the cross section ratio (per unit mass number) including higher order corrections. If, as speculated in this work, the HOC's do not alter R, then the two K factors should be the same.

One final remark regarding the QCD renormalization constant is in place. The effect of the Λ^2 choice is only minor in the calculation of R. However, for small values of x_F, x_T, and m^2 it may compete with f since an increase in either of them decreases the cross section in this region.

V. CONCLUSIONS

We have investigated the nuclear dependence of the Drell-Yan lepton pair production cross section ratio R to order α_s within the framework of the quark cluster model at RHIC energies. This ratio is essentially determined by the ocean quark distributions in the interacting nuclei and exhibits an EMC-like behavior based on which we

TABLE I. The exponent α showing the deviation of the Drell-Yan cross section in nucleus-nucleus collisions from that of proton-proton ones defined in Eq. (38). The upper value corresponds to the lowest f, calculated using Eq. (2), the largest a_3, and the smallest a_6. The opposite combination holds for the lower value. For this table we have taken $m = 5$ GeV but the results do not crucially depend on this choice.

	A	Z	$\alpha_{\rm (upper)}$	$\alpha_{\rm (lower)}$
d	2	1	0.895	0.884
Be	9	4	0.962	0.950
C	12	6	0.969	0.956
O	16	8	0.971	0.959
Cu	63	29	0.976	0.964
Sn	120	50	0.977	0.964
W	184	74	0.978	0.965
Au	197	79	0.978	0.965
U	238	92	0.978	0.965

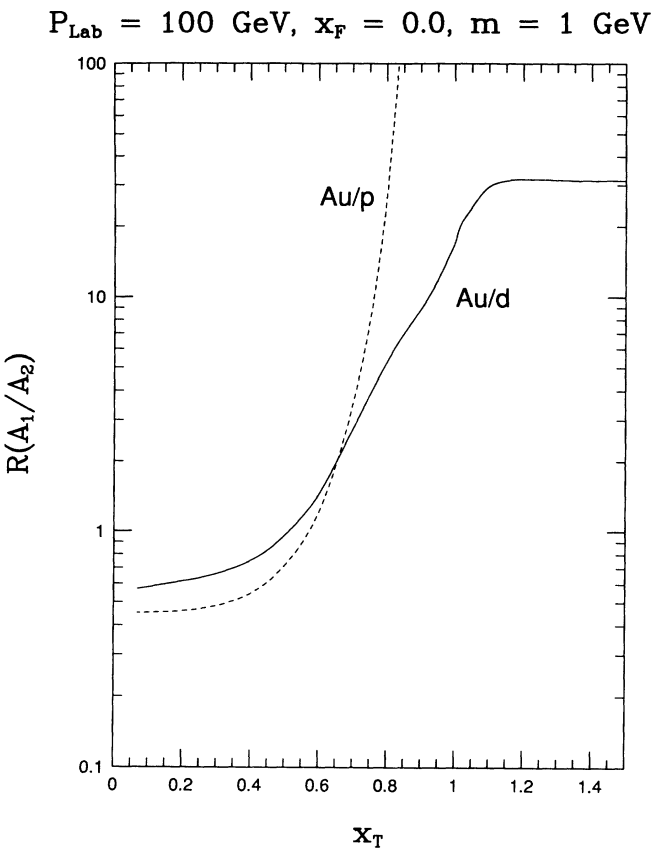

FIG. 10. Dependence of ratio of the Au to proton and deuterium lepton pair production on the lepton pair transverse momentum fraction (x_T) with $f_{Au} = 0.38$ and $f_d = 0.05$. The flattening of $R^{[A/d]}$ for large x_T is due to the $6q$ cluster component of deuterium.

can say that the nuclear ocean is expected to be reduced (*shadowed*) for small values of the pair longitudinal and transverse momentum and enhanced (*antishadowed*) for large values. The similar ratio of the integrated cross sections exhibits a less spectacular nuclear dependence which, however, is still stronger than that observed in hadron-nucleus collisions.

This calculation is potentially useful for the QGP search because it shows that low p_T lepton pairs emanating from the first stage of the collision will be produced at reduced rates per unit mass number at RHIC. This may enhance the detectability of Drell-Yan pairs from the QGP phase. It also shows that the heavy quarkonium peaks (in particular the Υ particle) must be measured relative to a background which is already modified by nuclear effects and implies that the quarkonium rates may also be altered due to modifications of the initial state parton momentum distributions.

On the other side of the spectrum, the high x_T or x_F lepton pairs are interesting in their own respect. Our predictions for the Drell-Yan process in heavy ion collisions are a consequence of the already established EMC effect which we attribute to modifications of the nonperturbative parton distributions in the nucleus relative to those of unbound nucleons. The high x_T rise of R is difficult to observe experimentally due to very low interaction rates in this region. However, given the RHIC anticipated peak luminosity which is of order 10^{26} cm^{-2} sec^{-1} we expect approximately 1000 lepton pairs per unit x_F and m^2 in the vicinity of $x_F = 0.60$ and $m = 1$ GeV per year of RHIC operation. We believe this is a tractable rate. For slightly higher x_F the second rise of R should become visible.

In closing we would like to emphasize that high energy heavy ion collisions are an important field to apply and test QCD and to further study nuclear effects that have already been observed in lepton and hadron interactions with nuclei.

The author wishes to express his gratitude to Dr. S. A. Shabalovskaya for useful discussions.

[1] S. D. Drell and T. M. Yan, Phys. Rev. Lett. **25**, 316 (1970).

[2] H. D. Politzer, Nucl. Phys. **B129**, 301 (1977).

[3] G. T. Bodwin, Phys. Rev. D **31**, 2616 (1985), has presented a detailed analysis of the QCD corrections to the Drell-Yan process proving that factorization holds for all order leading twist contributions and has included extensive references on the subject; J. C. Collins, D. E. Soper, and G. Sterman, Phys. Lett. **134B**, 263 (1984); W. W. Lindsay, D. A. Ross, and C. T. Sachrajda, Nucl. Phys. **B214**, 61 (1983); **B222**, 189 (1983).

[4] European Muon Collaboration, J. J. Aubert *et al.*, Phys. Lett. **123B**, 123 (1983); Nucl. Phys. **B259**, 189 (1985); **B272**, 158 (1986); A. Bodek *et al.*, Phys. Rev. Lett. **50**, 1431 (1983); **51**, 534 (1983); R. Arnold *et al.*, *ibid.* **52**, 727 (1984); G. Bari *et al.*, Phys. Lett. **163B**, 282 (1985); A. Benvenuti *et al.*, Phys. Lett. B **189**, 483 (1987); European Muon Collaboration, J. Ashman *et al.*, Z. Phys. C **57**, 211 (1993).

[5] T. Kitagaki *et al.*, in Proceedings of the Electronuclear Physics with Internal Targets Conference, Stanford, 1989; P. R. Norton (unpublished), p. 95; Rutherford Laboratory Report No. RL-85-054, 1985; T. Sloan, CERN Report No. EP/86-111, 1986.

[6] A. Bodek, S. Dasu, and S. Rock, Report No. SLAC-PUB-5598, 1991; New Muon Collaboration, P. Amaudruz *et al.*, Phys. Lett. B **295**, 159 (1992).

[7] A. Bodek and J. Ritchie, Phys. Rev. D **23**, 1070 (1981); **24**, 1400 (1981).

[8] C. A. Garcia Canal, E. M. Santangelo, and H. Vucetich, Phys. Rev. Lett. **53**, 1430 (1984); A. V. Kotikov, Report No. JINR-E2-88-140, 1988; L. P. Kaptari and A. Y. Umnikov, Report No. IC-92-151, 1992.

[9] F. Close, R. Jaffe, R. Roberts, and G. Ross, Phys. Rev. D **31**, 1004 (1985); F. Close, Nucl. Phys. **A478**, 407 (1988).

[10] E. Berger and F. Coester, Phys. Rev. D **32**, 1071 (1985).

[11] A. Mueller and J. Qiu, Nucl. Phys. **B268**, 427 (1986); J. Qiu, *ibid.* **B291**, 746 (1987).

[12] H. Pirner and J. Vary, Phys. Rev. Lett. **46**, 1376 (1981); C. Carlson and J. Havens, *ibid.* **51**, 261 (1983); M. Sato, S. A. Coon, H. J. Pirner, and J. P. Vary, Phys. Rev. C **33**, 1062 (1986).

[13] J. Dias de Deus, M. Pimenta, and J. Varela, Z. Phys. C **26**, 109 (1984); L. N. Epele, H. Fanchiotti, and C. A. Garcia Canal, J. Phys. G **15**, 583 (1989).

[14] K. E. Lassila and U. P. Sukhatme, Phys. Lett. B **209**, 343 (1988); Int. J. Mod. Phys. A **4**, 613 (1991).

[15] The Fermi motion is usually included by convoluting the cross section with the nucleon momentum distribution which, being the square of the magnitude of the nucleon wave function, is also responsible for the formation of multiquark clusters [A. N. Petridis (unpublished)].

[16] A. Harindranath and J. P. Vary, Phys. Rev. D **34**, 3378 (1986); K. E. Lassila, A. N. Petridis, C. E. Carlson, and U. P. Sukhatme, in *Proceedings of the Rice Meeting of the Division of Particles and Fields*, edited by B. Bonner and H. Miettinen (World Scientific, Teaneck, NJ, 1990), p. 593; K. E. Lassila, U. P. Sukhatme, A. Harindranath, and J. P. Vary, Phys. Rev. C **44**, 1188 (1991).

[17] A. N. Petridis, Ph.D. thesis, Iowa State University, 1992.

[18] P. Bordalo *et al.,* Phys. Lett. B **193**, 368 (1987); D. Alde *et al.,* Phys. Rev. Lett. **64**, 2479 (1990).

[19] K. E. Lassila, A. N. Petridis, U. P. Sukhatme, and G. Wilk, Phys. Lett. B **297**, 191 (1992); A. N. Petridis, C. E. Carlson, K. E. Lassila, and U. P. Sukhatme, in *Proceedings of the Vancouver Meeting of the Division of Particles and Fields*, edited by D. Axen, B. Bryan, and M. Comyn (World Scientific, Teaneck, NJ, 1991).

[20] A. N. Petridis, K. E. Lassila, and J. Vary, Phys. Rev. D **47**, 1906 (1993).

[21] E. Shuryak, Yad. Fiz. **28**, 796 (1978) [Sov. J. Nucl. Phys. **28**, 408 (1978)]; E. L. Feinberg, Nuovo Cimento A **34**, 391 (1976).

[22] The gluon distributions in QGP must be different from those of nucleons altering, in this way, the quarkonium production cross section in addition to possible screening, formation length modifications, and absorption phenomena.

[23] C. E. Carlson, K. E. Lassila, and U. P. Sukhatme, Phys. Lett. B **263**, 277 (1991).

[24] K. E. Lassila, A. N. Petridis, U. P. Sukhatme, and G. Wilk, Phys. Lett. B **297**, 191 (1992).

[25] According to M. Sawicki (private communication) since, in principle, x does not apply to all the components of parton the four-momentum, it should be defined using light-cone variables as $(k^0 + k^3)/(P^0 + P^3) \equiv (k^+/P^+)$, where P is the cluster four-momentum. Then the intrinsic transverse momentum of the partons can also be introduced and x is no longer identical to x_{Bj}.

[26] F. Halzen and D. Scott, Phys. Rev. D **18**, 3378 (1978).

[27] J. Kubar, M. Bellac, J. Meunier, and G. Plaut, Nucl. Phys. **B175**, 251 (1980).

[28] J. Badier *et al.,* Z. Phys. C **26**, 489 (1985).